

# Displacement Talbot lithography: a new method for high-resolution patterning of large areas

Harun H. Solak,\* Christian Dais, and Francis Clube

*Eulitha AG, 5232 Villigen PSI, Switzerland*

*\*harun.solak@eulitha.com*

**Abstract:** Periodic micro and nano-structures can be lithographically produced using the Talbot effect. However, the limited depth-of-field of the self-images has effectively prevented its practical use, especially for high-resolution structures with periods less than 1 micrometer. In this article we show that by integrating the diffraction field transmitted by a grating mask over a distance of one Talbot period, one can obtain an effective image that is independent of the absolute distance from the mask. In this way high resolution periodic patterns can be printed without the depth-of-field limitation of Talbot self-images. For one-dimensional patterns the image obtained is shown to be related to the convolution of the mask transmission function with itself. This technique, which we call Displacement Talbot Lithography (DTL), enables high-resolution photolithography without the need for complex and expensive projection optics for the production of periodic structures like diffraction gratings or photonic crystals. Experimental results showing the printing of linear gratings and an array of holes on a hexagonal lattice are presented.

©2011 Optical Society of America

**OCIS codes:** (050.2770) Gratings; (050.5298) Photonic crystals; (090.1970) Diffractive optics; (110.5220) Photolithography; (110.6760) Talbot and self-imaging effects.

---

## References and links

1. R. D. Piner, J. Zhu, F. Xu, S. H. Hong, and C. A. Mirkin, ““Dip-Pen” nanolithography,” *Science* **283**(5402), 661–663 (1999).
  2. S. R. J. Brueck, “Optical and interferometric lithography—nanotechnology enablers,” *Proc. IEEE* **93**(10), 1704–1721 (2005).
  3. T. A. Savas, M. L. Schattenburg, J. M. Carter, and H. I. Smith, “Large-area achromatic interferometric lithography for 100 nm period gratings and grids,” *J. Vac. Sci. Technol. B* **14**(6), 4167–4170 (1996).
  4. S. Y. Chou, P. R. Krauss, and P. J. Renstrom, “Imprint of sub-25nm vias and trenches in polymers,” *Appl. Phys. Lett.* **67**(21), 3114–3116 (1995).
  5. W. H. F. Talbot, “Facts relating to optical science,” *Philos. Mag.* **9**, 403–405 (1836).
  6. D. J. Shir, S. Jeon, H. Liao, M. Highland, D. G. Cahill, M. F. Su, I. F. El-Kady, C. G. Christodoulou, G. R. Bogart, A. V. Hamza, and J. A. Rogers, “Three-dimensional nanofabrication with elastomeric phase masks,” *J. Phys. Chem. B* **111**(45), 12945–12958 (2007).
  7. D. C. Flanders, A. M. Hawryluk, and H. I. Smith, “Spatial period division – a new technique for exposing sub-micrometer linewidth periodic and quasi periodic patterns,” *J. Vac. Sci. Technol.* **16**(6), 1949–1952 (1979).
  8. C. Zanke, M. H. Qi, and H. I. Smith, “Large-area patterning for photonic crystals via coherent diffraction lithography,” *J. Vac. Sci. Technol. B* **22**(6), 3352–3355 (2004).
  9. H. H. Solak, and Y. Ekinci, “Achromatic spatial frequency multiplication: a method for production of nanometer-scale periodic structures,” *J. Vac. Sci. Technol. B* **23**(6), 2705–2710 (2005).
  10. H. H. Solak, “A system and a method for generating periodic and/or quasi-periodic pattern on a sample.” Int'l. patent 1810085 (16 March 2011).
  11. J. W. Goodman, *Introduction to Fourier Optics* (McGraw-Hill Book Co., 1968), p. 48.
  12. Y. Bourgin, Y. Jourlin, O. Parriaux, A. Talneau, S. Tonchev, C. Veillas, P. Karvinen, N. Passilly, A. R. Md Zain, R. M. De La Rue, J. Van Erps, and D. Troadec, “100 nm period grating by high-index phase-mask immersion lithography,” *Opt. Express* **18**(10), 10557–10566 (2010).
  13. K. Knop, “Rigorous diffraction theory for transmission phase gratings with deep rectangular grooves,” *J. Opt. Soc. Am.* **68**(9), 1206–1210 (1978).
  14. D. M. Tennant, T. L. Koch, P. P. Mulgrew, R. P. Gnall, F. Ostermeyer, and J.-M. Verdiell, “Characterization of near field holography grating masks for optoelectronics fabricated by electron beam lithography,” *J. Vac. Sci. Technol. B* **10**(6), 2530–2535 (1992).
-

## 1. Introduction

Periodic patterns such as linear gratings or two-dimensional arrays of holes on a square grid are required for many current and emerging applications. Diffraction gratings for spectroscopy, fiber Bragg gratings, wire-grid polarizers, photonic crystals for improving light extraction from LEDs, anti-reflection structures, plasmonic color filters, bio-sensor arrays, nano-wire growth templates are examples in an ever growing list of such applications. An examination of the patterns required for these different fields reveals several common features. Firstly, the resolution defined in terms of the lattice constant of the periodic structure, is generally in the 100 nm – 1 μm range. Secondly, many applications require patterning of surfaces which are not very flat or clean. One of the most important examples for such non-ideal surfaces is encountered in the printing of photonic crystal patterns on LED wafers. High temperature deposition processes involved in LED fabrication cause the substrates to be bowed and deformed. In addition, the same processes lead to incorporation of particulates on LED wafers. These issues have presented considerable difficulties for methods requiring intimate contact or have limited depth-of-field, as we explain below. Thirdly, the nanostructures usually need to be formed on large areas at a relatively low cost.

Over the years projection optical lithography has served the patterning needs of the microelectronics industry but it is not always suitable for the types of applications mentioned above because of depth of focus limitations and more importantly, because of its high cost. Proximity lithography is a relatively lower cost technology but the resolution available is typically limited to about 0.5-1 μm. The lower end of this range is extremely difficult to reach and it is only possible in a strict contact regime, which is not generally accessible for routine use. The serial electron beam lithography method is too slow and hence not suitable for high-volume manufacturing. Likewise, other scanning probe techniques such as dip-pen lithography do not have the necessary throughput [1]. Interference lithography, in which two or more mutually coherent UV beams interfere to generate periodic patterns can be used to print periodic structures over large areas [2,3]. Whereas resolution is not an issue for this method, it too does not avail itself to volume production because the optical configuration needs to be modified for printing different patterns and strict control and stabilization of the environment are required for forming stationary fringe patterns. Nano-imprint method has

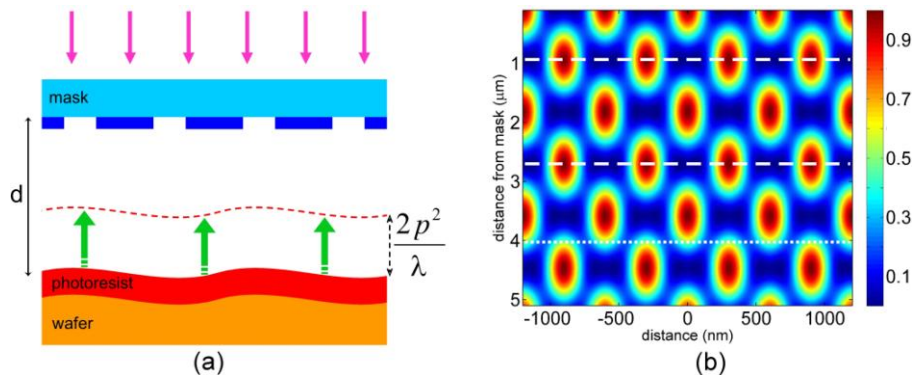


Fig. 1. (a) Schematic diagram illustrating the new DTL method. The photoresist-coated substrate is moved towards the mask by one Talbot period during the exposure. (b) Calculated intensity distribution after a linear grating. Two self images are marked with dashed lines at distances 0.9 μm and 2.7 μm from the grating. The dotted horizontal line below marks the position of a Talbot sub-image, with twice the frequency of the original grating.

spurred extensive development efforts due to its potential for large-area patterning at low cost [4]. However, difficulties remain with respect to particulate contamination, substrate topography and the presence of a residual polymer layer. Therefore, currently there is a need for a robust, high-throughput lithography method that has the capability to produce sub-

micron resolution periodic patterns over large areas at a low cost. The Displacement Talbot Lithography (DTL) method that we introduce here has such a potential.

## 2. Theory of operation of Displacement Talbot Lithography

The Talbot effect is a well-known phenomenon in which a periodic structure (grating) is illuminated with monochromatic collimated light to form self-images of the grating pattern at periodic intervals after the grating [5]. For a linear grating, the self-images repeat with a Talbot period of approximately  $2p^2/\lambda$  where  $p$  is the grating period and  $\lambda$  is the wavelength. At certain distances corresponding to integer fractions of the Talbot period, Talbot sub-images are formed whose frequency is a multiple of the grating frequency. Use of self-images and sub-images have been the subject of many studies to print high-resolution structures [6,7]. The depth of field (DOF) of the Talbot images scales with the square of the grating period. For example, for a pattern with period 400 nm illuminated by light with wavelength 365 nm, the DOF is only about 50 nm. This small DOF requires very precise positioning of the wafer with respect to the mask [8] and it excludes the use of non-flat substrates or thick photoresists. Recently, a modified version of Talbot lithography has been reported in which the DOF problem is overcome by illuminating the mask with a beam having a broad spectral bandwidth [9]. With this technique the different wavelength components of the transmitted light-field overlap and beyond a certain distance from the mask they form an image that is invariant with respect to further increase in distance. In this article, we demonstrate that a similar result can be obtained by illuminating the mask with a monochromatic beam and changing the distance (or gap) between the mask and the substrate during the exposure by one Talbot period [10] as schematically illustrated in Fig. 1(a). This displacement leads to the recording of an effective image that is independent of the absolute value of the gap. It is further shown that the obtained image is different from a self-image. For a one-dimensional grating pattern, it is related to the convolution of the grating transmission function with itself.

The DTL concept is further explained with the aid of the calculated Talbot pattern shown in Fig. 1(b). In this example, a linear grating with 600 nm period is illuminated at normal incidence with light of wavelength 365 nm. The grating consists of equal width (300 nm) opaque lines and clear spaces. The transmitted intensity distribution repeats itself with a Talbot period of 1.8  $\mu\text{m}$  in the direction away from the grating. Two consecutive self-images separated by this distance are indicated by dashed lines. A phase-shifted self-image occurs halfway between the dashed lines, which is displaced by half the grating period in the lateral direction. Frequency-doubled Talbot sub-images are also present between the self-images, one of which is marked with a dotted line. The DTL integral is performed over a complete Talbot period. While the starting position of this integral has no influence on the outcome, the integral may be performed between the two dashed lines. It will therefore have contributions from the whole range of lateral intensity distributions that is present over one Talbot period; including the self-image, the phase-shifted self-image and sub-images. By inspecting the intensity distribution it can be readily concluded that the integrated distribution has half the period of the grating in the mask. This is confirmed by the theoretical analysis that follows.

The transmission function,  $T(x)$  of a one-dimensional grating positioned in the  $xy$  plane of a Cartesian coordinate system with lines lying parallel to the  $y$  axis can be written in terms of its Fourier series as

$$T(x) = \sum_m A_m \exp(i \frac{2m\pi}{p} x), \quad (1)$$

where  $p$  is the pattern period. When the grating is illuminated with a plane monochromatic wave with unit amplitude propagating in the  $z$ -direction, the electric field  $E(x,z)$  in the transmitted light-field can be found using the angular spectrum method [11] through

$$E(x, z) = \sum_m A_m \exp(i \frac{2m\pi}{p} x) \exp\left(i \frac{2\pi}{\lambda} z \sqrt{1 - \frac{\lambda^2 m^2}{p^2}}\right). \quad (2)$$

In general the above summation runs from minus to plus infinity but we only have to consider orders for which  $m\lambda < p$ , since higher orders are evanescent and decay very quickly in the near field of the grating. We further assume that  $m\lambda$  is much smaller than the period  $p$  for all orders where the Fourier coefficient  $A_m$  has an appreciable value. With this simplification we can use the paraxial approximation and calculate the field intensity as

$$I(x, z) = \sum_{m,n} A_m A_n^* \exp(i \frac{2\pi}{p} (m-n)x) \exp\left(i \frac{2\pi}{\tau} z (m^2 - n^2)\right), \quad (3)$$

where  $\tau = 2p^2/\lambda$ , is the Talbot period. Inspection of the above equation shows that the intensity distribution is periodic along the direction of propagation  $z$  with a period  $\tau$ , which is the basis of the Talbot effect. Now, let us consider a photoresist-coated substrate being moved with constant speed in the  $z$  direction by one Talbot period, i.e. from a starting position  $z_0$  to  $z_0 + \tau$ , while being exposed to the diffraction field. The photoresist layer acts as an integrating detector so the dose deposited in the photoresist (per unit time) as a function of position  $x$  can be found by integrating the expression for intensity in Eq. (3) as

$$D(x) = \sum_{m,n} A_m A_n^* \exp(i \frac{2\pi}{p} (m-n)x) \int_{z_0}^{z_0+\tau} \exp\left(i \frac{2\pi}{\tau} z (m^2 - n^2)\right) dz. \quad (4)$$

We first observe that the integral in the above equation is non-zero only when  $m = \pm n$ . Most interestingly, because of the periodicity of the intensity along the  $z$  direction, the resulting distribution  $D(x)$  is independent of the starting position  $z_0$ . This means that we can position the photoresist coated substrate at any distance  $z_0$  from the grating and always deposit the same dose distribution in our photoresist film. Now, we investigate further what this distribution will resemble. Through straightforward manipulation of Eq. (4) and considering that the integral is non-zero only when  $m = \pm n$  we reach the following expression for the dose distribution:

$$D(x) = \tau \sum_m |A_m|^2 - \tau |A_0|^2 + \tau S(2x), \quad (5)$$

where

$$S(x) = \sum_m A_m A_{-m}^* \exp\left(i \frac{2\pi m x}{p}\right), \quad (6)$$

is the convolution of the grating transmission  $T(x)$  with itself as defined by the following relation

$$S(x) = \int_{-p/2}^{p/2} T(x') T^*(x-x') dx'. \quad (7)$$

We note that, this result is valid for all one-dimensional transmission functions  $T(x)$ , irrespective of whether they are real, complex, symmetric or not. Therefore, notwithstanding the first two terms in Eq. (5), which are constants, we conclude that for a one-dimensional grating the DTL exposure prints the self-convolution function of the mask. Equation (5) further tells us that the resulting image  $D(x)$  has twice the frequency of the grating, due to the factor 2 in the argument of the function  $S(2x)$  in that equation.

Next, we consider the impact of a crucial assumption that we have made in the foregoing derivation. In reality, the printed function  $D(x)$  has limited resolution due to the finite wavelength which limits the number of propagating orders in the summations in Eq. (2) to 5, as previously discussed; whereas the true Fourier series representation of the convolution

function given in Eq. (6) has no such restriction on the order index  $m$ . Therefore, in general the experimentally obtained distribution is an approximation of the convolution function, the correspondence becoming more accurate when the period to wavelength ratio is increased. In addition, we note that when the wavelength is close to the pattern period such that there are few diffraction orders, the paraxial approximation gives less reliable results. In this regime electromagnetic simulation methods should rather be used to calculate the transmission of the illuminated grating structure and the propagation of light beyond it.

The above result relating the DTL image to the self-convolution function of the mask transmission is not in general valid for two-dimensional gratings, such as an array of holes on a square or hexagonal lattice. While a detailed discussion of the DTL image formed by a 2D grating is beyond the scope of this article, it can be stated that a DOF-free image can be obtained using the DTL technique for both one and two-dimensional gratings due to the basic fact that the integral of a periodic function (i.e. the diffraction field behind a grating) is independent of the limits of the integral as long as it is performed over one period. We should also note that the DTL image is imperfectly formed at the edges of the grating pattern because the diffracted orders do not fully overlap at the plane of the substrate. Assuming that the image is dominated by the first-order diffracted beams, then the width of this region is approximately given by  $d\lambda/p$ , where  $d$  is the gap between the mask and grating. This region whose width is on the order of the gap  $d$ , should be considered in the application of the DTL technique (as in other Talbot-based lithography methods), but for many applications this region is very small in relation to the size of the pattern and so can be largely neglected.

### 3. Experimental demonstration

In a first set of experiments to validate the DTL concept, masks with linear gratings having periods 500 nm, 600 nm and 700 nm were prepared on fused silica substrates. The line patterns were etched into the substrates to provide an approximately  $180^\circ$  phase shift between the light transmitted by the lines and spaces. We made rough measurements of the relative diffraction efficiency into the first versus zeroth orders (higher orders are absent due to the period-wavelength ratio). In all cases the zeroth order diffraction was stronger than the first order because the grating parameters deviated from those of an ideal phase-shift grating designed for minimizing the zeroth order. In view of this, one would expect a strong Talbot effect, i.e. a strong dependence of the intensity distribution on distance from the mask due to the interference between the zeroth and first order diffracted beams. For the DTL exposures the starting substrate-to-mask distance was adjusted to be in the range 30–50  $\mu\text{m}$ , but no effort was made to ensure a more precise gap setting. The wafer, which was mounted on a vacuum chuck, was then displaced by one Talbot period while illuminating the mask with a monochromatic UV beam. The displacement was in the range 1.3  $\mu\text{m}$  to 2.7  $\mu\text{m}$  depending on the grating period. Individual exposures took 2-3 min. in order to deliver the necessary dose to the  $\sim 1$   $\mu\text{m}$ -thick i-line sensitive photoresist. Standard photoresist processing was employed. The resulting patterns in photoresist on Si wafers are shown in Fig. 2. The pattern

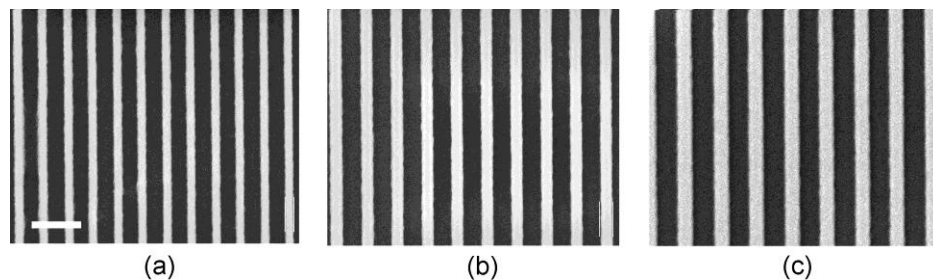


Fig. 2. SEM images of high-resolution linear grating patterns fabricated in photoresist using the DTL method. The periods of the patterns shown in (a)-(c) are 250 nm, 300 nm and 350 nm, whereas the periods of the respective patterns in the mask were 500 nm, 600 nm and 700 nm. The DTL exposure therefore produces a frequency multiplication. The scale bar is 500 nm long.

periods are 250 nm, 300 nm and 350 nm, corresponding to half the periods of the respective patterns in the mask. Reproducible and high-quality lithographic results were obtained irrespective of the starting gap, which demonstrated the large DOF despite the strong Talbot effect. Using the DTL technique it is therefore not necessary to reduce the zeroth order to a fraction of the first order diffraction as is generally required in phase-shift lithography [12]. This is a major advantage for high-resolution lithography especially because the reduction of zeroth order diffraction becomes increasingly more difficult as the period of the phase grating approaches the wavelength [13]. In addition, unlike in phase-shift techniques [14], the presence of higher diffraction orders (e.g. second or higher orders) is not detrimental in the DTL technique; therefore the period range is not restricted.

Another experiment was designed to demonstrate the patterning of 2D structures with the DTL method. A mask with the pattern design shown in Fig. 3a covering an area of 46mm x 46mm was manufactured on a fused silica plate. Clear holes were opened in a 100 nm thick Cr film to form an amplitude mask. Exposures were performed on photoresist-coated Si wafers using collimated illumination at normal incidence. The mask-to-wafer distance was again varied by one Talbot period during the exposure. The hole pattern was uniformly and reproducibly printed into the photoresist despite the initial gap varying by several microns over the pattern area. In some cases the resultant pattern was etched into the underlying Si substrate. An SEM image of an array of holes etched into the Si substrate showing the high quality of the obtained pattern is presented in Fig. 3b. A photograph of one of the 4" wafers patterned with the DTL technique is shown in Fig. 3c.

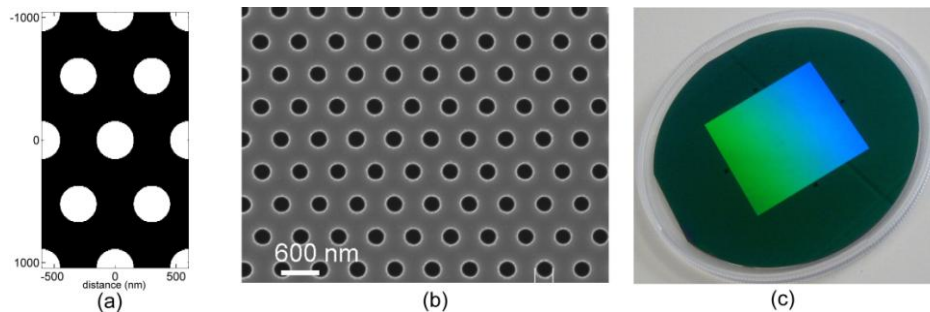


Fig. 3. Application of the DTL method to a periodic pattern with hexagonal symmetry. (a) Schematic view of the mask pattern which consists of clear circular apertures in a thin opaque layer. (b) SEM image of a pattern of 300 nm-diameter holes with 600 nm period obtained by a DTL exposure and transferred into a silicon wafer by reactive ion etching. (c) Photograph of the photonic crystal pattern printed in photoresist on a 4" Si wafer.

#### 4. Conclusions

The DTL method introduced here is based on the familiar and powerful concepts of using a photomask and UV exposure of a photoresist to create patterns. Presence of a gap between the mask and wafer ensures safe use of the mask for many exposures. Patterns can be uniformly printed over large surfaces with significant topography because the effective image does not depend on the distance of the substrate from the mask. Many different pattern types such as 1D linear gratings and 2D arrays with hexagonal or square symmetry can be printed using the same exposure system by simply changing the mask. DTL patterns can be accurately overlaid over existing patterns using standard alignment techniques of proximity photolithography. The resolution limit is set only by the wavelength, with the minimum achievable pitch being close to one half of the wavelength. Structures with periods below 100 nm would be possible using deep-UV illumination sources such as an ArF lasers operating at 193 nm.

#### Acknowledgements

Part of the theoretical work reported here was performed by one of the authors (HHS) while he was with the Paul Scherrer Institute, Switzerland.